The Astrophysical Journal Letters, 891:L21 (7pp), 2020 March 1 https://doi.org/10.3847/2041-8213/ab7931

Rapid Evolution of Type II Spicules Observed in Goode Solar Telescope On-disk H_α Images

Vasyl Yurchyshyn[1], Wenda Cao[1], Valentina Abramenko[2], Xu Yang[1], and Kyung-Suk Cho[3,4]
[1] Big Bear Solar Observatory, New Jersey Institute of Technology, 40386 North Shore Lane, Big Bear City, CA 92314, USA; vasyl.yurchyshyn@njit.edu
[2] Crimean Astrophysical Observatory of Russian Academy of Science, Nauchny, Bakhchisaray, Russia†
[3] Space Science Division, Korea Astronomy and Space Science Institute, Daejeon 305-348, Republic of Korea
[4] Department of Astronomy and Space Science, University of Science and Technology, Daejeon 305-348, Republic of Korea
Received 2019 December 5; revised 2020 February 20; accepted 2020 February 23; published 2020 March 4

Abstract

We analyze ground-based chromospheric data acquired at a high temporal cadence of 2 s in wings of the H_α spectral line using the Goode Solar Telescope operating at the Big Bear Solar Observatory. We inspected a 30 minute long $H_\alpha-0.08$ nm data set to find that rapid blueshifted H_α excursions (RBEs), which are a cool component of type II spicules, experience very rapid morphological changes on timescales of the order of 1 s. Unlike typical reconnection jets, RBEs very frequently appear in situ without any clear evidence of H_α material being injected from below. Their evolution includes inverted "Y," "V," "N," and parallel splitting (doubling) patterns as well as sudden formation of a diffuse region followed by branching. We also find that the same feature may undergo several splitting episodes within about a 1 minute time interval.

Unified Astronomy Thesaurus concepts: Quiet solar chromosphere (1986); Solar coronal heating (1989)

1. Introduction

Large- and small-scale jets and upflows observed in the lower atmosphere of quiet Sun (QS) areas are considered to play an important role in the transfer of mass and energy from the dense chromosphere into the corona. However, their origin and connection to the dynamics of the magnetic fields are not well understood and explored.

Type II spicules were first discovered in off-limb *Hinode* data (De Pontieu et al. 2007a). They are short-lived (<100 s), thin (<0.″7) structures seen everywhere in *Hinode* Ca II images that show high Doppler velocities (50–150 km s^{-1}, De Pontieu et al. 2007a) and return flows (Pereira et al. 2014). When observed in *IRIS* data, they show higher apparent speeds of 80–300 km s^{-1} (Tian et al. 2014; Narang et al. 2016). Type II spicules are omnipresent and they carry a large amount of magnetic energy (De Pontieu et al. 2007b, 2012; McIntosh et al. 2011; Liu et al. 2019).

Type II spicules were found to have on-disk counterparts. They have been identified with Ca II "straws" and rapid blueshifted excursions (RBEs) seen in Ca II 854.2 nm (Langangen et al. 2008) and H_α lines on the solar disk (e.g., Rutten 2006; Rouppe van der Voort et al. 2009; Kuridze et al. 2015). Here we use the term type II spicules, when referring to these events as a class (e.g., when discussing their formation mechanisms or models) and we use the term RBE when referring to their H_α component observed on the disk. Recently, Rutten et al. (2019) speculated that RBEs may also display return flows. Sekse et al. (2013) utilized 0.88 s temporal cadence data to find that the RBE lifetime ranges from 5 to 60 s and their transverse velocities may reach up to 55 km s^{-1}. Wang et al. (1998) described a new type of small-scale chromospheric event, which they called upflows, and suggested that these events may be fueling coronal heating. They were linked to magnetic reconnection between the existing network fields and opposite-polarity internetwork fields and ephemeral regions. Chae et al. (1998) attempted to associate the upflows with SUMMER UV explosive events and magnetic reconnection in QS areas. Lee et al. (2000) reported that the majority of the upflow events show absorption only in the blue wing of the H_α line, which is similar to the RBEs (e.g., Langangen et al. 2008).

Some type II spicules appear to show twisting motions (e.g., Tomczyk et al. 2007; De Pontieu et al. 2012) or doubling (Suematsu et al. 2008), and they have been used as tracers for Alfvénic waves (De Pontieu et al. 2007b). Their identification in *IRIS* and AIA images and the increased line broadening suggests that they are heated to at least the transition region temperatures (e.g., De Pontieu et al. 2007a, 2007b, 2009, 2012; Henriques et al. 2016). When observed in the *Hinode* Ca II band, they show fading on timescales of an order of tens of seconds (De Pontieu et al. 2007b). Type II spicules and RBEs are subject to various high-frequency oscillations (e.g., Okamoto & De Pontieu 2011; Sekse et al. 2013). Although it is not clear what drives type II spicules, two energy sources may be considered: leakage of p-mode waves into the chromosphere or release of magnetic energy either via release of magnetic tension Martínez-Sykora et al. (2017), oscillatory reconnection (McLaughlin et al. 2012), or magnetic reconnection (Yurchyshyn et al. 2013; Deng et al. 2015; Samanta et al. 2019). Judge et al. (2012) argued that spicules II could be warps in 2D sheet-like structures, while Zhang et al. 2012 questioned the existence of spicules II as a distinct class altogether.

The formation process of type II spicules is thought to affect the corona by generating shocks, flows, waves, and currents, which can be linked to other phenomena such as the red–blue asymmetries observed in UV data as well as propagating coronal disturbances observed with the 17.1 and 19.3 nm *SDO*/AIA channels (e.g., Chae et al. 1998; Martínez-Sykora et al. 2018). Their detailed physical cause and role in providing mass and energy to the corona remain largely unknown. The related difficulties in the interpretation of solar data mainly arise from

† While the AAS journals adhere to and respect UN resolutions regarding the designations of territories (available at http://www.un.org/press/en), it is our policy to use the affiliations provided by our authors on published articles.

the limited spatial resolution and complexity of the chromosphere (e.g., Leenaarts et al. 2012). They appear in regions of seemingly unipolar magnetic fields often surrounding clusters of photospheric bright points (e.g., McIntosh & De Pontieu 2009). De Pontieu et al. (2011) suggested that they may be a product of reconnection. Yurchyshyn et al. (2013) reported that the occurrence of packets of type II spicules is generally correlated with the appearance of new, mixed, or unipolar fields in close proximity to network fields. These authors also suggested that emerging fields may introduce rapid reconfiguration of equilibrium in the preexisting fields, which may further lead to both small-scale (component) reconnection and high-frequency MHD waves. Detection of kinked and/or inverse "Y" shaped RBEs further confirms this conclusion. Recently, Samanta et al. (2019) observed that RBEs appeared in the Goode Solar Telescope (GST) data within minutes after opposite-polarity magnetic flux appeared around a cluster of dominant polarity.

De Pontieu et al. (2017) used 2.5D radiative MHD simulations to show that spicules can be driven by ambipolar diffusion resulting from ion-neutral interactions. Martínez-Sykora et al. (2017) further advanced the study and found that simulated spicules occur when magnetic tension is amplified and transported upward through interactions between ions and neutrals or ambipolar diffusion. The tension is impulsively released to drive flows, heat plasma (through ambipolar diffusion), and generate Alfvénic waves. The magnetic tension is introduced in the system through new flux emergence that undergoes reconnection with the ambient fields. It is important to stress that the simulated spicules were not accelerated by the reconnection event. Nevertheless, none of the current models can explain all of the observed properties of type II spicules and RBEs including their omnipresence (De Pontieu et al. 2007a; Pereira et al. 2012), temperature, and the associated wave energy (e.g., Liu et al. 2019).

2. Data

On 2019 June 7 GST, Cao et al. (2010) and Goode et al. (2010) acquired QS data near the disk center at heliocentric-Cartesian position (−115″, 135″) with the aid of an adaptive optics system. We only used data from the Visible Imaging Spectrometer (VIS), which utilizes a Fabry–Pérot interferometer with a bandpass of 0.008 nm and the possibility to shift the bandpass by 0.2 nm around the H_α line center. The pixel scale was set to 0.″027 and the field of view (FOV) of the imager was 75″ × 64″. RBEs display notable Doppler shift and line broadening and are best seen in the blue wing of the H_α spectral line. Generally speaking the number of RBEs seen in the FOV decreases with the increasing distance from the H_α line center. However, when observing closer to the line center the FOV is contaminated by overlying fibrils with their own flows. To acquire high cadence data we limited our choice of usable wavelengths to one spectral position (H_α−0.08 nm). We also acquired a short series of H_α−0.08 and H_α+0.08 nm pairs that allowed us to produce H_α 0.08 nm Doppler maps at a 5 s cadence. The original data was acquired in bursts of 25 frames each. All bursts were speckle reconstructed using the Wöger & von der Lühe (2007) technique to produce the final H_α−0.08 nm images with 2 s cadence, which were aligned and destretched to remove residual image distortion due to seeing and telescope jitter. The intensity of each image was adjusted to the average level of the data set.

3. Results

Here we discuss data for 12 RBE events that showed very rapid and distinct evolutionary patterns. Figure 1 shows evolution of events 1–6. Note that the bright lanes seen in the background are chains of bright points seen in the intergranular lanes. Event E1 lasted for about 30 s and started as broadening of the preexisting feature (solid line in 51:31 panel and arrow in 51:39 panel) followed by a double RBE that appeared to be joined at the top thus forming the inverted "Y" pattern. The two "legs" that extend down from the location indicated by the red arrow in 51:50 panel (dashed lines) were developed during this process and they appear in H_α to be extending downward toward the photosphere. The feature widening was not accompanied by an injection of chromospheric plasma observable in the H_α line into the volume as is typical for a chromospheric jet. Sekse et al. (2012) reported that the lower endpoints of Ca II 854.2 nm component of RBEs are located closer to the network, so that injection of cool plasma may still occur without being detectable in the H_α line. We also point out the sudden appearance (<8 s) and equally rapid disappearance (<5 s) of an RBE feature (not related to E1) seen at the bottom of 51:39–51:55 panels of event E1. Other similar examples will be discussed further in the text. Event E3 (bottom row) is another example of RBE doubling although this feature was much broader, darker, and longer living.

Event E2 displays a different type of evolution where an existing RBE (solid line in 51:47 panel) suddenly dimmed and became fuzzy in the midsection. In each of these panels, the solid line marks the initial position of the RBE as it was recorded at 51:47. Very faint dark strands then appeared on both sides of the RBE. To enhance the strands, we subtracted the background and the residual image in the 52:19 panel shows the enhanced features (arrows). The strands appeared to be moving away from the original RBE at a rate of about 25 km s^{-1}, while the main feature remained stationary (solid line in 52:27).

Event E4 represents a "fractured" RBE formed after it suddenly darkened, and broke into two branches displaced in the horizontal direction (arrow in 01:05 panel). Note that the lower part at that moment is no longer cospatial with the initial position (yellow line). In a matter of seconds the upper branch disappeared, while the lower part extended upward thus forming a new RBE feature displaced by about 0.″3 from the initial position over a period of time of about 5–7 s resulting in the displacement rate of about 30–50 km s^{-1}.

Events E5 and E6 represent other cases of dimmed and diffuse evolution of RBEs. Similar to the E2 event, a faint side line appeared on one side of E5 (arrow in 01:41 panel), and it soon developed into a regular RBE feature. Event E6 developed a very compact, well defined, oval-shaped diffuse region (arrow in 02:15 panel) of about 0.″2 Mm wide and 1 Mm long. The lower branch of the RBE (below the diffuse region) showed later displacement by about 0.2 Mm. It is not clear whether the upper part was displaced as well or a new feature formed at that location. Similarly to the previous cases the displacement rate was estimated to be about 30–50 km s^{-1}.

In Figure 2 we show the same QS area with three "N" pattern features. The arrow in the 58:41 panel (top row) shows an "N" pattern consisting of two vertical and one slanted RBE streaks. This pattern typically starts from one slanted feature (E7, the yellow line in the 58:15 panel) that rapidly evolves first into an x-configuration and then into an "N" configuration as the new features form and separate. The "N" pattern then changes into

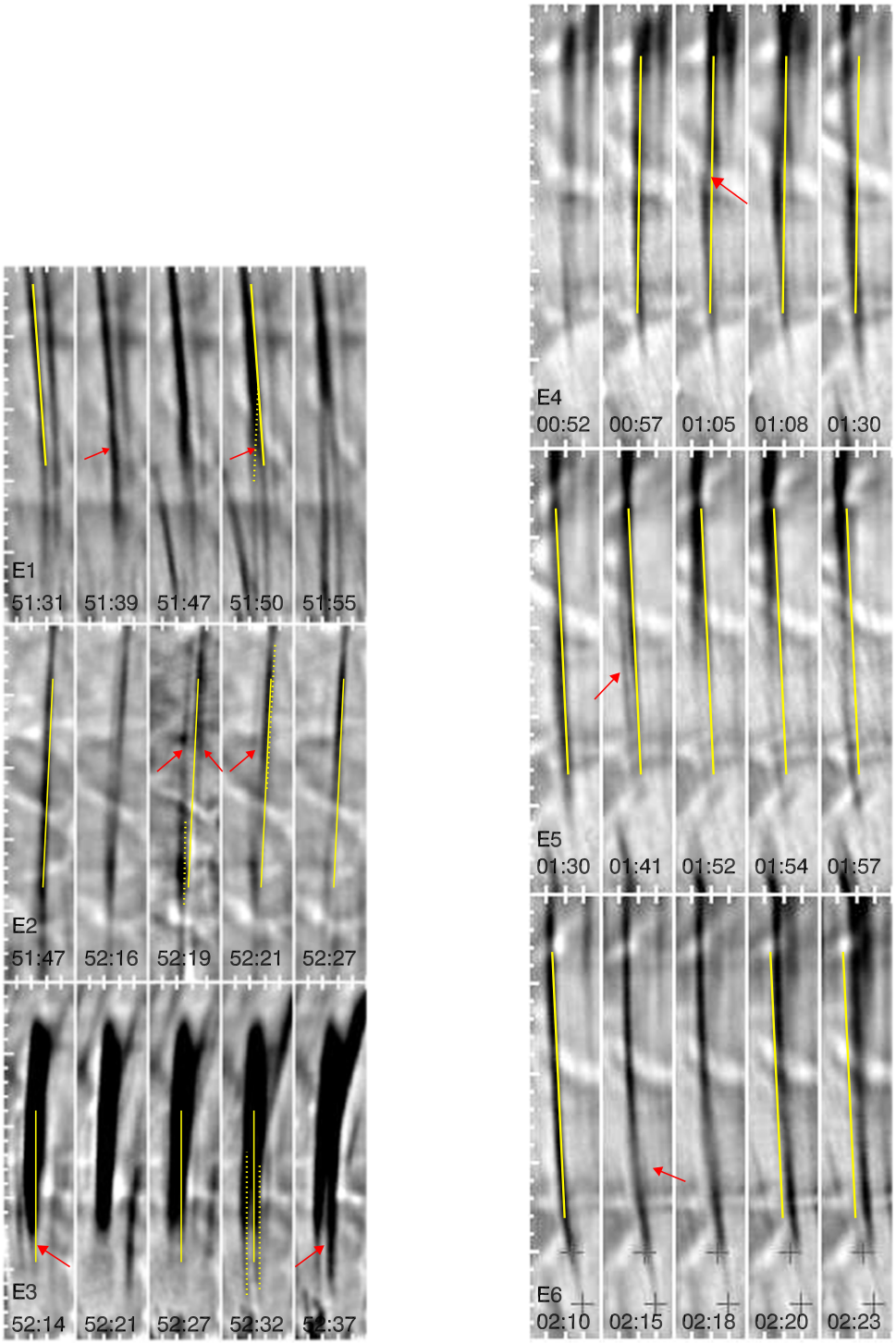

Figure 1. Evolution of events 1–6 as seen in GST/VIS $H_{\alpha}-0.08$ nm data. The over-plotted solid yellow lines indicate the initial position of the evolving RBE, while dashed lines highlight newly formed features. Arrows point toward various features that are discussed in the text. Note that the format of the time stamp at the bottom of each panel is MM:SS and the short tick marks separate 0.2 Mm (0.″275) intervals. Crosses in the E6 panels mark two initial positions of the RBE endpoint and are plotted to ease comparison.

what appears to be a "kinked" spicule (58:52), which gradually straightens (58:57 panel). However, it is not clear if that "kinked" RBE was indeed one feature or a composition of several smaller components.

Apart from the most prominent RBE transformation cases that we describe here, there also are other sudden in situ appearances of RBEs. Comparison of the 58:15 and 58:25 panels of event E7 shows that several dark striations have appeared within a 10 s time interval on the left side of the yellow line shown in the 58:15 panel. Similarly, several new features appeared in the same area between 58:38 and 58:49 panels. A new, "Y" shaped feature is visible in the center of the 59:44 panel of event E9 that was not present yet in the 59:30 panel.

Evolution of event E8 is similar to E7 with the only distinction that the "N" pattern (arrow in 59:07 panel) evolved

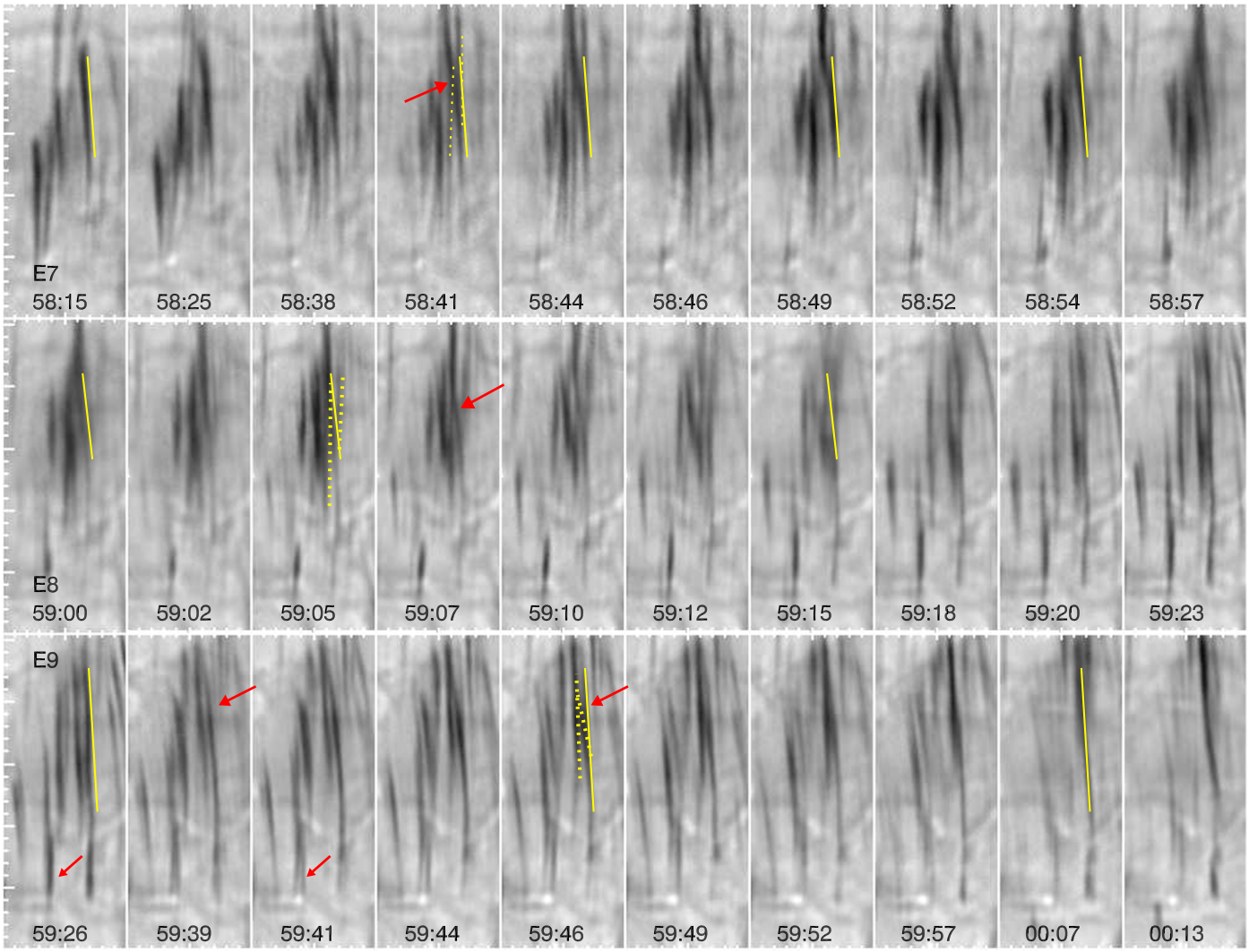

Figure 2. Same as in Figure 1 but for events 7–9.

into two, a well defined double RBE feature with component separation of about 0.3 Mm. Event E9 is another example of the "N" pattern that involved an RBE with swaying motion (compare 59:26–59:41 panels). We should note that the swaying RBE was formed only about 10 s prior to the E8 event.

We also note an RBE event that started as a single streak (red arrow in the lower left corner of the 59:26 panel of Figure 2) and within 15 s evolved into a double feature with its lower endpoints at the opposite sides of a developing brightening and the upper endpoints still joined at a distance of about 1 Mm from the brightening (panel 59:39). Note that the brightening was not yet present in the 59:26 panel. This conjoined feature was observed to completely separate 5 s later (panel 59:44).

Finally, in Figure 3 we show a "V" splitting pattern (E10) where a preexisting RBE (black arrow and yellow solid line in 06:18 panel) evolves into a double feature that appear to be joined at their roots (opposite of the inverse "Y" splitting discussed above). The transition from a single to a double feature occurred within a 6 s interval (compare 06:23 and 06:29 panels). We should note that one of the double spicules split again following the "V" pattern (E12, 07:00 panel) and the new features later separated into nearly parallel structures (07:16 panel). The E11 event showed a parallel splitting or doubling. The original feature seen in 06:34 panel (solid yellow line) widened and 6 s later it is already seen split (06:42 panel). The components were moving away from each other and faded in about 10 s.

The last event in our series, E12 (arrows in 06:13, 06:44, and 07:08 panels), is quite different from the previous ones. It resembles an inverted "Y" (or anemone, e.g., Shibata et al. 2007) jet. It started before 06:08 and first appeared as a regular RBE. However, it had a much longer lifetime and was extending upward gradually developing into a typical reconnection jet with clear footpoint separation of about 500 km (07:24 panel).

While these evolutionary patterns may, generally speaking, result from overlapping of multiple features, we argue that the cases considered here are not contaminated by that effect. Our arguments are primarily based on the fact that the evolving features showed structural changes (widening, darkening, or disappearance) before splitting into two parts or doubling. In most cases no features other than the evolving one were present at the scene at the beginning of the RBE transformation. To demonstrate the difference, we point to the fan-shaped system of loops seen in Figure 3 (arrow in 06:10 panel) that showed rapid transverse displacement. The system was observed moving in the background behind the jet (arrow 06:13 panel) without any detectable interaction with it or other stationary

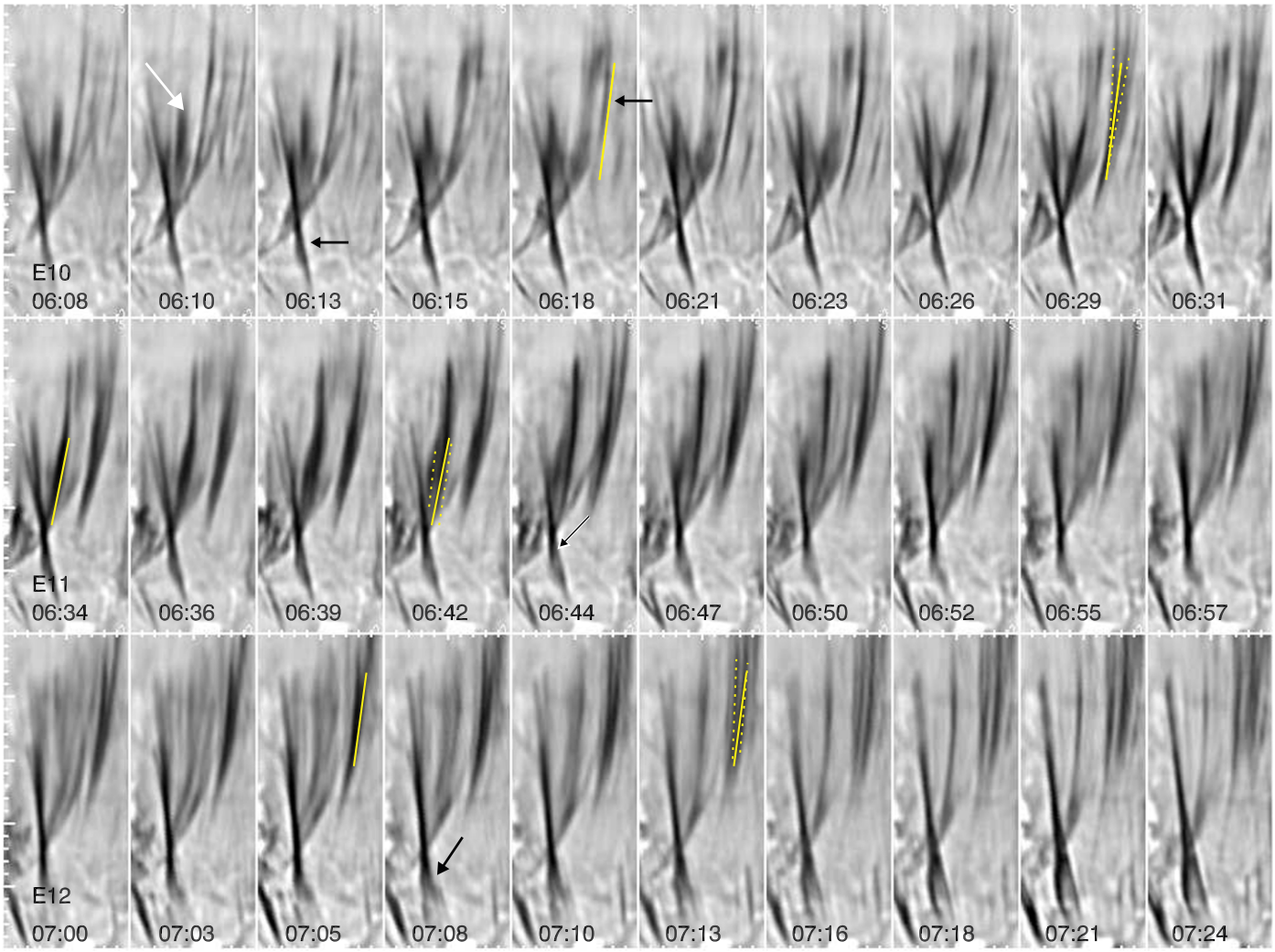

Figure 3. Same as in Figure 1 but for events 10–12.

features. In contrast, quite often a complex "N" pattern develops from a single stationary feature initially present in the FOV (e.g., E7 in Figure 2).

Figure 4 shows $H_\alpha \pm 0.08$ nm images (left and right columns) and the corresponding Doppler image (middle) of evolving RBEs at three instances. The Dopplergrams of two splitting RBEs show that prior to and during the event, the evolving features appeared blueshifted in the GST/VIS instrument. However, we did not observe detailed spectra of the event, which is needed to perform an accurate analysis of the line-of-sight speeds associated with these RBE transformations.

4. Summary and Discussion

We inspected a 30 minute long data set and found that the RBE transformations described above are very frequent and ubiquitous. Although each new individual feature followed its own unique evolutionary path, they often exhibit group behavior (McIntosh et al. 2011) when several strands follow coherent swaying motions. We thus summarize our findings as follows: (i) very frequently RBEs suddenly appear in situ as nonextending plasma structures without prior H_α features and clear evidence of H_α emitting material being injected from below; (ii) they rapidly evolve on timescales of the order of 1 s; (iii) their evolution includes inverted "Y, "V, "N," or parallel splitting (doubling) as well as sudden formation of a diffuse region followed by branching; and (iv) the same feature may undergo several splitting episodes within about a 1 minute time interval.

Sekse et al. (2013) interpreted the sudden appearance of RBEs over their full length as a combination of field-aligned flows, transverse swaying, and torsional motions (e.g., De Pontieu et al. 2012). De Pontieu et al. (2011) noted that the appearance of AIA type II spicules is delayed relative to the corresponding H_α feature (also Pereira et al. 2014). At the same time Sekse et al. (2013) reported that Ca II 854.2 nm RBEs may appear earlier than their H_α component. Skogsrud et al. (2015) reported that when Ca II spicules fade from the passband they continue to be visible in other "hotter" spectral lines. These data suggest that spicules are heated during their lifetime. This also implies that the H_α component of type II spicules (RBEs) considered here may appear in the FOV before any other hotter component as a result of heating of cool plasma detected in Ca II 854.2 nm (Sekse et al. 2013). However, their sudden in situ appearance in the $H_\alpha - 0.08$ nm spectral window via transformation of existing features does not seem to be consistent with any of the models that interpret these events as jets originating in the lower chromosphere (e.g., González-Avilés et al. 2018). On the contrary, in some cases we seem to

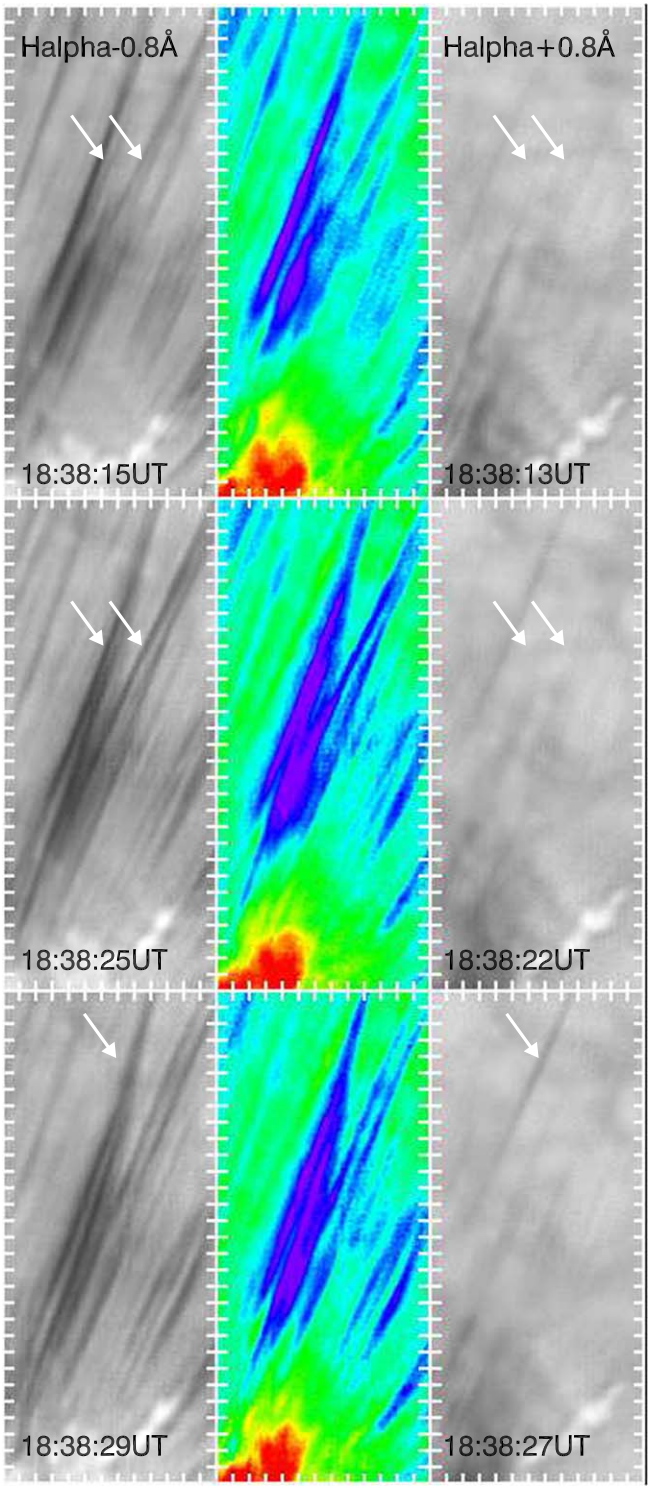

Figure 4. $H_\alpha-0.08$ nm (left), $H_\alpha+0.08$ nm (right) and the corresponding H_α Doppler image (middle). The tick marks separate 0.2 Mm ($0\farcs275$) intervals.

observe the opposite effect: during their transformation process some $H_\alpha-0.08$ nm RBEs are seen extending downward toward the photosphere.

Recently, Cho et al. (2019) reported on a new type of faint chromospheric jet detected at a limb in Ca II *Hinode* images. These jets exhibit an average speed of about 132 km s^{-1} and an average lifetime of 20 s, ranging from 11 to 36 s. These new limb jets could be related to the short-lived RBEs discussed here. These jets appear to originate 2–3 Mm above the limb, which roughly places them at the top of H_α RBEs.

Samanta et al. (2019) identified magnetic flux cancellations at the footpoint of some analyzed RBEs. Two events considered in the present study do exhibit morphological features and evolutionary pattern consistent with the flux cancellation scenario. On the other hand, new flux emergence may trigger enhanced spicule activity observed as bursts of RBEs (Yurchyshyn et al. 2013; Samanta et al. 2019). These may suggest that in addition to directly driving the RBEs, flux emergence may also cause both restructuring of coronal fields and wave generation (e.g., Isobe et al. 2008; van Ballegooijen et al. 2011; Srivastava et al. 2017), which in turn may be responsible for the rapid RBE transformations reported here. Furthermore, waves are also generated by vigorous turbulent flows (e.g., Aschwanden et al. 2018a; Liu et al. 2019). The MHD waves experience reflection near the TR and propagate downward (Okamoto & De Pontieu 2011). All these may create complex and dynamic interactions when coronal fields within a flux tube attempt to counter the destabilizing driving force and injection of energy (Aschwanden et al. 2018b) via multiple small-scale reconnection events occurring throughout the volume. Additionally, the short lifetime and sudden appearance of these events may be a manifestation of the sheet-like structures as conjectured by Judge et al. (2012).

The events presented here resemble the well-known idea of intertwined and tangled magnetic field lines (Parker 1989). The criss-crossing patterns formed by RBEs are also somewhat similar to the synthetic emission of UV strands heated via multiple reconnections of tangled field lines within a flux tube (see Figures 5–7 in Pontin et al. 2017). However, while it is tempting to interpret the RBE transformations as driven by component magnetic reconnection, we should be mindful that according to Pontin et al. (2017) the appearance of energy release regions associated with reconnection in a braided magnetic structure may be wavelength and geometry dependent. The data presented here were acquired in only one, very narrow spectral range and multiwavelength data sets need to be analyzed to learn about the temperature and flow patterns associated with the locations where RBE transformations occur and to offer a plausible explanation.

BBSO operation is supported by NJIT and US NSF AGS-1821294 grants. GST operation is partly supported by the Korea Astronomy and Space Science Institute (KASI), Seoul National University, the Key Laboratory of Solar Activities of Chinese Academy of Sciences (CAS), and the Operation, Maintenance and Upgrading Fund of CAS for Astronomical Telescopes and Facility Instruments. V.Y. acknowledges support from NSF AST-1614457, AFOSR FA9550-19-1-0040, and NASA 80NSSC17K0016, 80NSSC19K0257, and 80NSSC20K0025 grants. X.Y. was supported by NSF 1821294, 1614457, and National Science Foundation of China 11729301 grants. K-S.C. acknowledges support from KASI under the R&D program "Development of a Solar Coronagraph on International Space Station" (project No. 2020-1-850-02) supervised by the Ministry of Science and ICT.

Facility: GST.

ORCID iDs

Vasyl Yurchyshyn https://orcid.org/0000-0001-9982-2175
Wenda Cao https://orcid.org/0000-0003-2427-6047
Valentina Abramenko https://orcid.org/0000-0001-6466-4226
Xu Yang https://orcid.org/0000-0002-3238-0779
Kyung-Suk Cho https://orcid.org/0000-0003-2161-9606

References

Aschwanden, M. J., Gošic, M., Hurlburt, N. E., & Scullion, E. 2018a, ApJ, 866, 73
Aschwanden, M. J., Scholkmann, F., Béthune, W., et al. 2018b, SSRv, 214, 55
Cao, W., Gorceix, N., Coulter, R., et al. 2010, AN, 331, 636
Chae, J., Wang, H., Lee, C.-Y., Goode, P. R., & Schühle, U. 1998, ApJL, 504, L123
Cho, K.-S., Cho, I.-H., Nakariakov, V. M., et al. 2019, ApJL, 877, L1
De Pontieu, B., Carlsson, M., Rouppe van der Voort, L. H. M., et al. 2012, ApJL, 752, L12
De Pontieu, B., Martínez-Sykora, J., & Chintzoglou, G. 2017, ApJL, 849, L7
De Pontieu, B., McIntosh, S., Hansteen, V. H., et al. 2007a, PASJ, 59, 655
De Pontieu, B., McIntosh, S. W., Carlsson, M., et al. 2007b, Sci, 318, 1574
De Pontieu, B., McIntosh, S. W., Carlsson, M., et al. 2011, Sci, 331, 55
De Pontieu, B., McIntosh, S. W., Hansteen, V. H., & Schrijver, C. J. 2009, ApJL, 701, L1
Deng, N., Chen, X., Liu, C., et al. 2015, ApJ, 799, 219
González-Avilés, J. J., Guzmán, F. S., Fedun, V., et al. 2018, ApJ, 856, 176
Goode, P. R., Yurchyshyn, V., Cao, W., et al. 2010, ApJL, 714, L31
Henriques, V. M. J., Kuridze, D., Mathioudakis, M., & Keenan, F. P. 2016, ApJ, 820, 124
Isobe, H., Proctor, M. R. E., & Weiss, N. O. 2008, ApJL, 679, L57
Judge, P. G., Reardon, K., & Cauzzi, G. 2012, ApJL, 755, L11
Kuridze, D., Henriques, V., Mathioudakis, M., et al. 2015, ApJ, 802, 26
Langangen, Ø., De Pontieu, B., Carlsson, M., et al. 2008, ApJL, 679, L167
Lee, C.-Y., Chae, J., & Wang, H. 2000, ApJ, 545, 1124
Leenaarts, J., Carlsson, M., & van der Voort, L. R. 2012, ApJ, 749, 136
Liu, J., Nelson, C., Snow, B., Wang, Y., & Erdélyi, R. 2019, NatCo, 10, 3504
Martínez-Sykora, J., De Pontieu, B., De Moortel, I., Hansteen, V. H., & Carlsson, M. 2018, ApJ, 860, 116
Martínez-Sykora, J., De Pontieu, B., Hansteen, V. H., et al. 2017, Sci, 356, 1269
McIntosh, S. W., & De Pontieu, B. 2009, ApJL, 706, L80
McIntosh, S. W., De Pontieu, B., Carlsson, M., et al. 2011, Natur, 475, 477
McLaughlin, J. A., Verth, G., Fedun, V., & Erdélyi, R. 2012, ApJ, 749, 30
Narang, N., Arbacher, R. T., Tian, H., et al. 2016, SoPh, 291, 1129
Okamoto, T. J., & De Pontieu, B. 2011, ApJL, 736, L24
Parker, E. N. 1989, SoPh, 121, 271
Pereira, T. M. D., De Pontieu, B., & Carlsson, M. 2012, ApJ, 759, 18
Pereira, T. M. D., De Pontieu, B., Carlsson, M., et al. 2014, ApJL, 792, L15
Pontin, D. I., Janvier, M., Tiwari, S. K., et al. 2017, ApJ, 837, 108
Rouppe van der Voort, L., Leenaarts, J., De Pontieu, B., Carlsson, M., & Vissers, G. 2009, ApJ, 705, 272
Rutten, R. J. 2006, in ASP Conf. Ser. 354, Solar MHD Theory and Observations: A High Spatial Resolution Perspective, ed. J. Leibacher, R. F. Stein, & H. Uitenbroek (San Francisco, CA: ASP), 276
Rutten, R. J., Rouppe van der Voort, L. H. M., & De Pontieu, B. 2019, A&A, 632, A96
Samanta, T., Tian, H., Yurchyshyn, V., et al. 2019, Sci, 366, 890
Sekse, D. H., Rouppe van der Voort, L., & De Pontieu, B. 2012, ApJ, 752, 108
Sekse, D. H., Rouppe van der Voort, L., & De Pontieu, B. 2013, ApJ, 764, 164
Shibata, K., Nakamura, T., Matsumoto, T., et al. 2007, Sci, 318, 1591
Skogsrud, H., Rouppe van der Voort, L., De Pontieu, B., & Pereira, T. M. D. 2015, ApJ, 806, 170
Srivastava, A. K., Shetye, J., Murawski, K., et al. 2017, NatSR, 7, 43147
Suematsu, Y., Ichimoto, K., Katsukawa, Y., et al. 2008, in ASP Conf. Ser. 397, First Results From Hinode, ed. S. A. Matthews, J. M. Davis, & L. K. Harra (San Francisco, CA: ASP), 27
Tian, H., DeLuca, E. E., Cranmer, S. R., et al. 2014, Sci, 346, 1255711
Tomczyk, S., McIntosh, S. W., Keil, S. L., et al. 2007, Sci, 317, 1192
van Ballegooijen, A. A., Asgari-Targhi, M., Cranmer, S. R., & DeLuca, E. E. 2011, ApJ, 736, 3
Wang, H., Johannesson, A., Stage, M., Lee, C., & Zirin, H. 1998, SoPh, 178, 55
Wöger, F., & von der Lühe, O. 2007, ApOpt, 46, 8015
Yurchyshyn, V., Abramenko, V., & Goode, P. 2013, ApJ, 767, 17
Zhang, Y. Z., Shibata, K., Wang, J. X., et al. 2012, ApJ, 750, 16